2

Amphiphilic DNA Anchoring to Membranes

Parts of this chapter were published in: Adv. Healthc. Mater. 2019, 1900389.

2.1 Introduction

The biological membrane, known as plasma membrane, separates the cell cytosol from the extracellular environment. The basic building block of the mammalian cell membrane is a semi permeable lipid bilayer. Phospholipids, composed of a polar head with phosphate group and two hydrophobic fatty acid tails, contribute as a major part to the membrane. They form a bilayer by assembling hydrophobic tails together while their hydrophilic heads facing either cytosol or extracellular fluid. Most of the phospholipids of the cell membrane are unsaturated. Cholesterol, another lipid component, is embedded between phospholipid molecules and regulates membrane stiffness and stability. Although the cell membrane is a closed, non leaky bilayer system, the individual phospholipid molecules are dynamic and mobile. They move freely in two dimensions, providing cell membrane with the fluidity. Cell membrane is not just a homogeneous unsaturated lipid bilayer. It also has certain lipids enriched domains called lipid raft. Cholesterol, sphingomyelin and tightly packed saturated phospholipids form these lipid rafts and they are more stable and less fluid than the rest of membrane.[1] When embedded with specific membrane proteins, these lipid rafts are essential for cellular functions such as signal transduction and endocytosis. Apart from lipids, cell membrane contains many proteins. These proteins make up about half of the cellular membrane by mass and are responsible for many membrane functions, like cell signaling,[2] cell-cell interactions and nutrient transportation.[3, 4] Some of the lipids, proteins and other membrane constituents recycle between the plasma membrane and intracellular endocytic compartments[5, 6] or between different cells within the body by extracellular vesicles, known as exosomes.

Similar with the cell membrane, liposome is a small synthetic spherical structure with an aqueous lumen sealed by a bilayer membrane. Its bilayer can be constructed from phospholipids and cholesterol, similar as a biological membrane. The composition of liposome bilayer determines its rigidity. Unsaturated phosphatidylcholine species (for instance, DOPC and DOPE) are more fluidic thus less stable as compared with saturated phospholipids with long acyl chains (DPPC as an example) which forms a rigid and rather impermeable bilayer structure.[7] Liposomes have been long used in the clinic as nanocarriers for drug delivery, due to

their biocompatibility, self-assembly property and high drug loading capacity.[8] Up to date, many liposome based products are available on the market for clinical application, e.g., Doxil®, Ambisome®, Onivyde™, etc.[9]. To further improve their colloidal stability and in vivo circulation time, conventional liposomes are then PEGylated by adding 5 mol% PEG-lipid to the total lipid content.[10, 11] Moreover, liposome membrane can be easily modified with many ligands, for instance DNA, peptides or other small molecules (**Fig. 2.1**).[12] As being highly programmable and functional, DNA is a quite attractive membrane modification. The most simple way to modify liposome surfaces with DNA is to anchor amphiphilic DNA to its bilayer by hydrophobic interaction between hydrophobic part of the amphiphilic DNA and membrane lipids.[13, 14, 15, 16, 17]

Previous reports of our group showed that dodec-1-yne-modified deoxyuridine nucleotides could be incorporated into common DNA sequences[18] and the resulting lipid DNA could be anchored to phospholipid-based liposome (DOPC, DOPE, cholesterol) membrane in a straightforward manner[19]. Therefore, as an extension of this work, we here explored the ability of lipid DNA anchoring to different formulations of liposomes, namely, liposome made from unsaturated phospholipids (DOPC:DOPE:cholesterol = 2:1:1), saturated phospholipids (DPPC:cholesterol = 2:1) and their PEGylated form. Besides this, we further challenged to anchor lipid DNA to a more complicated bilayer system: the cell membrane. To anchor DNA to membranes, oligonucleotides were conjugated with either four (U4T23, U4T) or six (U6T) lipid modified deoxyuridine nucleotides. Their sequences and the complementary sequences are detailed in **Table 2.1** and **Fig. 2.2a**.

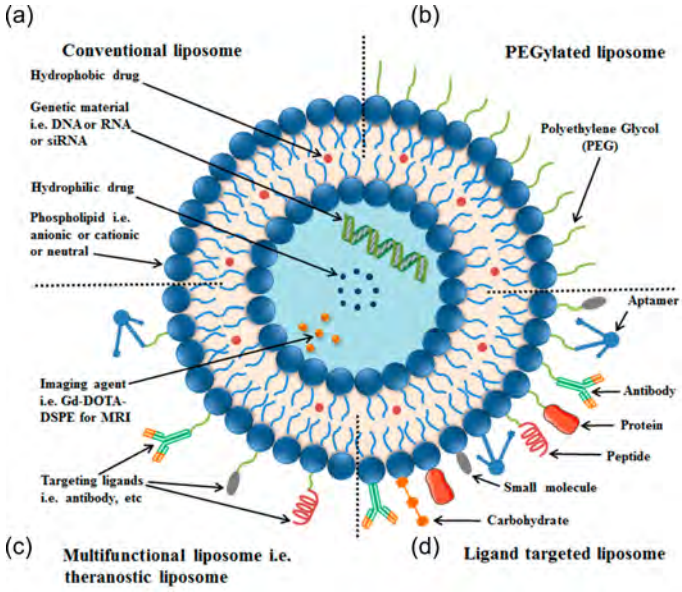

Figure 2.1 | Schematic illustration of liposome surface modification.[12] (a) Conventional liposome made of phospholipids; (b) PEGylated liposome contains a layer of polyethylene glycol (PEG) at the surface; (c) Targeted liposome contains a specific targeting ligand; (d) Multi-functional liposome.

2.2 Results and Discussions

2.2.1 Lipid DNA Anchoring to Liposome Membrane

To prove anchoring of lipid DNA to liposomal membranes, fluorescence resonance energy transfer (FRET) method established in previous work[19] was employed. Lipid DNA (U4T) was first anchored to the liposome membrane (incorporated with a fluorophore as an acceptor dye) and then hybridized with its complementary strand labeled with a donor dye. Hybridization should bring the donor and the acceptor dye close enough to initiate FRET, as illustrated in **Fig. 2.2b, (1)**.

Name	Sequence (5' to 3')	Modification
U4T23	**UUUU**TTTGGGGGTTGAGGCTAAGCCGA	3-FAM
U4T	**UUUU**GCGGATTCGTCTGC	None
U6T	**UUUUUU**GCGGATTCGTCTGC	None
CU4T FAM	GCAGACGAATCCGC	5-FAM
CU4T ATTO488	GCAGACGAATCCGC	3-ATTO488

Table 2.1 | Sequences and modifications of lipid DNA used in this chapter.

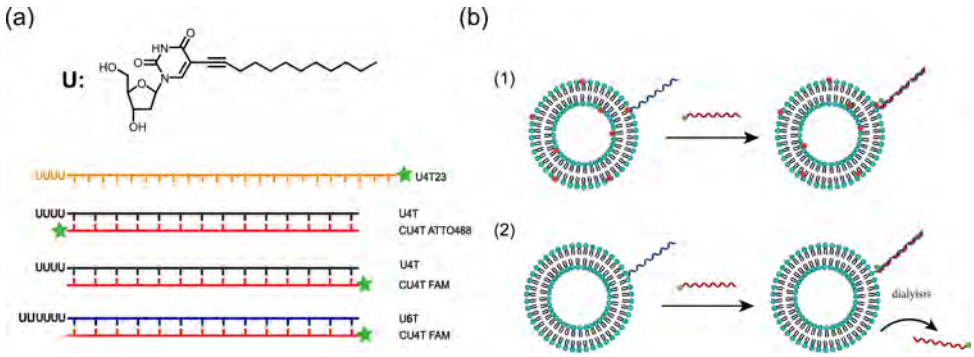

Figure 2.2 | (a) Schematic illustration of lipid DNA used in this chapter. **U** represents dodecyne modified deoxyuridine nucleotide. The green star symbolizes fluorophore-modified DNA strands. (b) Schematic illustration of lipid DNA anchoring proof and its quantification on liposomal membrane. (1) FRET between a donor dye (green dot) and an acceptor dye (red dot) occurred on liposome membrane upon hybridization of lipid DNA with its complementary strand. (2) Lipid DNA quantification on liposome membrane after dialysis purification.

For quantification of membrane anchored lipid DNA, after dialysis of free unhybridized strands, fluorescence intensity of the liposome solution was recorded and compared with a calibration curve of free complementary strand to calculate the membrane anchored lipid DNA and its hybridization efficiency, see **Fig. 2.2b, (2)**.

Lipid DNA Anchoring to Unsaturated Liposome

To prove the anchoring of U4T to the membrane of liposome made of unsaturated phospholipids, U4T was first anchored to the liposome (DOPC:DOPE:rhodamine-DHPE:cholesterol = 2:1:0.09:1, d = 100 nm). To do this, dried U4T was mixed with phospholipids in ethanol. After solvent evaporation, freeze-drying cycles and size reduction by extrusion, U4T anchored liposomes were prepared. The resulting liposomes were hybridized with a complementary DNA modified with ATTO488 at the 3' end (CU4T ATTO488). The hybridization of U4T and CU4T ATTO488 brought ATTO488 in close contact to rhodamine, initiating FRET. Upon lysis of the liposomes with 0.3% Triton X-100, the distance between ATTO488 and rhodamine increased, consequently decreasing the FRET efficiency, and hence proving the successful strand hybridization on the liposome surface (**Fig. 2.3a**). In addition, a gradual decrease of liposome surface zeta potential (**Fig. 2.13b**) was indicative of successful U4T anchoring and hybridization. We subsequently quantified DNA anchoring efficiency to the liposomal membrane by hybridizing U4T-anchored liposomes with CU4T FAM. After dialysis and removal of the non-hybridized components, FAM fluorescence intensity of the liposome in comparison with the calibration curve of free CU4T FAM allowed us to calculate the amount of CU4T FAM in the liposome solution (**Fig. 2.3b**). This amount corresponds to roughly half of the U4T initially employed in the functionalization process and is an expected value, as we suppose that lipid DNA also anchored to the inner leaflet of the liposome membrane, inaccessible to CU4T FAM hybridization. Based on **Eq. 2.1** and **2.2**, ca. 500 strands are estimated to be on each liposome surface.

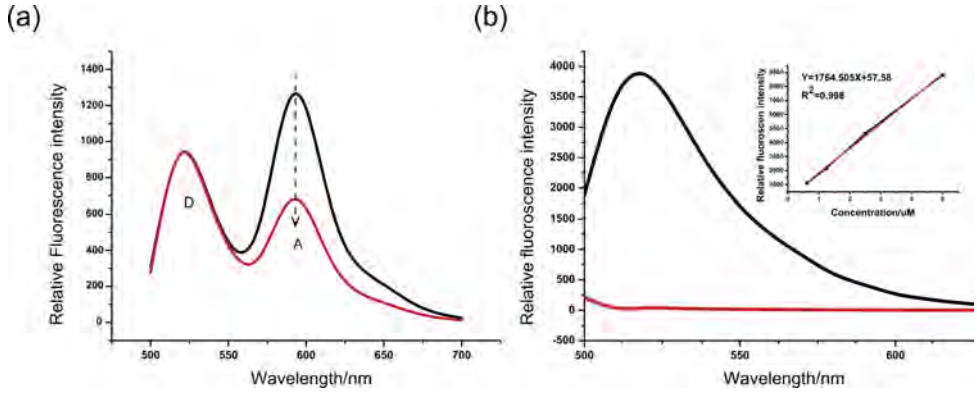

Figure 2.3 | Lipid DNA anchoring to unsaturated liposomal membrane. (a) FRET efficiency of ATTO488 and rhodamine occurred on liposome. After adding 0.3% Triton X-100, FRET efficiency decreased. D: maximum emission wavelength of donor dye ATTO488; A: maximum emission wavelength of acceptor dye rhodamine. Black curve: before Triton X-100 addition; red curve: after Triton X-100 addition. (b) Fluorescence intensity of CU4T FAM in liposome solution after dialysis of free CU4T FAM. Black curve: relative fluorescence intensity of U4T anchored liposome solution. Red curve: relative fluorescence intensity of non U4T anchored control liposome solution. Inset graph is the calibration curve of free CU4T FAM. Black: curve plotted from experimental data; red: fitted curve.

Lipid DNA Anchoring to Saturated Liposome

After confirming that U4T is able to anchor to unsaturated liposomes, we further tried to anchor it to a saturated liposome composition (DPPC:cholesterol = 2:1) with less membrane fluidity. Again, FRET of ATTO488 and rhodamine was used to prove anchoring. Quite unexpectedly, we noticed a very weak FRET signal as compared with that of unsaturated liposomes. After lysis with Triton X-100, instead of decreasing, acceptor rhodamine fluorescence intensity increased two fold (**Fig. 2.4a**). To address the reason for this behavior, rhodamine-DHPE incorporated liposomes wihout U4T anchoring were prepared and only negligible rhodamin signal was observed. However, after Triton X-100 treatment, its signal significantly increased up to 10 times (**Fig. 2.4b**). This measurement indicated that rhodamine-DHPE incorporated into DPPC liposome domains, thus its fluorescence was quenched due to the high local concentration. Because of this quenching effect, rhodamine-DHPE is not a suitable acceptor for DPPC liposomes. Therefore, another lipophilic fluorophore, Nile red was employed as the acceptor. After Triton X-100 lysis, decrease of Nile red signal and a large shift of its emission

peak was noticed (**Fig. 2.4c**). Whereas this is considered as an effect induced by Triton X-100, not by the FRET process, as this was also seen from a bare liposome with only Nile red embedded (**Fig. 2.4d**). We reasoned that Triton X-100 changes the environment of Nile red by which its fluorescence is strongly influenced. Besides, an increase of ATTO488 emission signal was seen, but it was decreased for the control liposome without U4T anchoring (**Fig. 2.4e**). This is an indication for the occurrence of FRET because after Triton X-100 addition, the liposomes disassembled and FRET from ATTO488 to Nile red disappeared, thus emission of ATTO488 itself increased which is not sensitive to the environmental polarity. In control liposomes, since there was no FRET, only decrease of ATTO488 could be seen as a result of sample dilution by Triton X-100. Although it is not easy to probe lipid DNA anchoring to saturated liposome by the FRET method, the direct quantification method by measuring fluorescent intensity of its complementary DNA could definitely imply its successful anchoring and hybridization. Thus, anchored U4T was quantified by hybridizing with CU4T FAM and a half anchoring to outer leaflet and full hybridization was also detected (**Fig. 2.4f**), as for the unsaturated liposome.

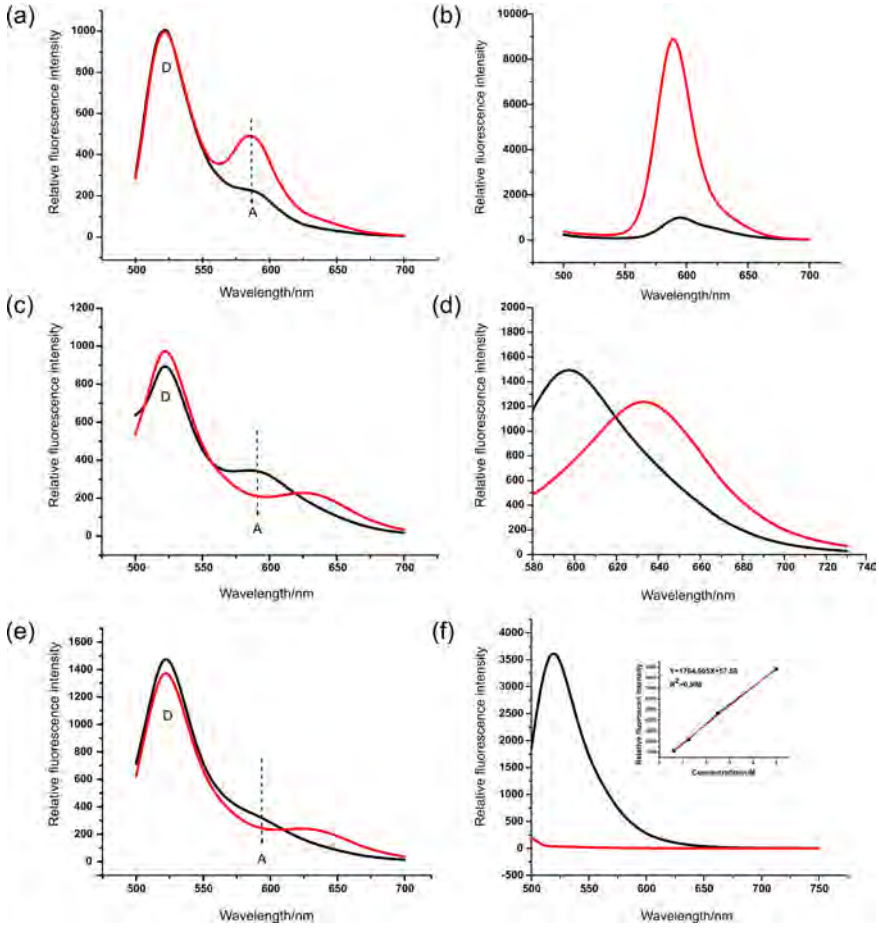

Figure 2.4 | Lipid DNA anchoring to DPPC liposomal membrane. (a) FRET phenomenon of ATTO488 and rhodamine on DPPC liposome. After adding 0.3% Triton X-100, rhodamine signal increased. D: maximum emission wavelength of donor dye ATTO488; A: maximum emission wavelength of acceptor dye rhodamine. Black curve: before Triton X-100 addition; red curve: after Triton X-100 addition. (b) rhodamine-DHPE signal change after DPPC liposome lysis. After 0.3% Triton X-100, rhodamine signal significantly increased. Black curve: before Triton X-100 addition; red curve: after Triton X-100 addition. (c) FRET phenomenon of ATTO488 and Nile red on DPPC liposome. D: maximum emission wavelength of donor dye ATTO488; A: maximum emission wavelength of acceptor dye Nile red. Black curve: before Triton X-100 addition; red curve: after Triton X-100 addition. (d) Decrease of Nile red signal and shift of its emission wavelength after adding 0.3% Triton X-100 to Nile red embedded DPPC liposome. (e) Excitation of Nile red incorporated DPPC liposome with no U4T anchoring. Black curve: before Triton X-100 addition; red curve: after Triton X-100 addition. (f) Fluorescence intensity of CU4T FAM in liposome solution after dialysis of free CU4T FAM. Black curve: relative fluorescence intensity of U4T anchored liposome solution. Red curve: relative fluorescence intensity of non U4T anchored control liposome solution. Inset graph is the calibration curve of free CU4T FAM. Black: curve plotted from experimental data; red: fitted curve.

Lipid DNA Anchoring to PEGylated Liposome

For therapeutic applications, liposomes are widely formulated with additional 5% PEG-lipid as PEGylation increases its circulation time and improves the enhanced permeation retention (EPR) effect. Thus, here we tested whether lipid DNA could also anchor to PEGylated liposomes with the hybridization method as shown above. The signal of CU4T FAM in U4T anchored liposome solution was extremely high whereas it was hardly detectable for the non-anchored control liposome in both PEGylated non-saturated (**Fig. 2.5a**) and saturated liposomes (**Fig. 2.5b**). Quantification of CU4T FAM signals indicated that PEG layer had no effect on U4T anchoring in these liposomes.

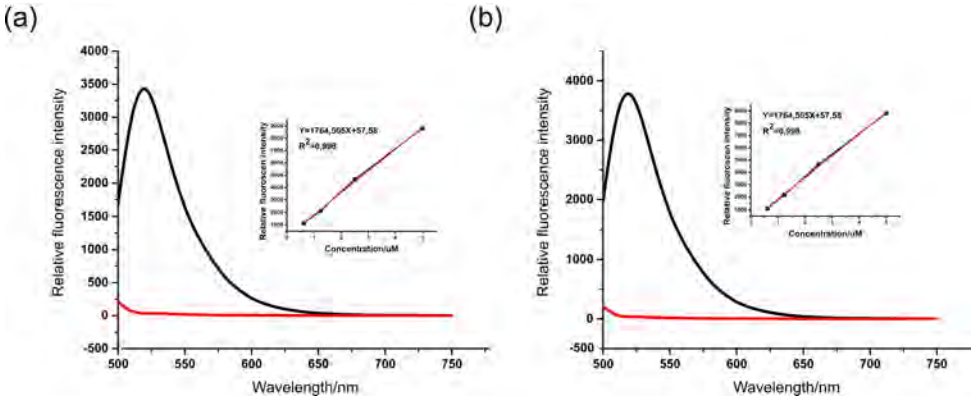

Figure 2.5 | Lipid DNA anchoring on PEGylated liposomal membrane. Fluorescence intensity of CU4T FAM from the liposome solution after dialysis of free CU4T FAM. Black curve: relative fluorescence intensity of U4T anchored liposome solution. Red curve: relative fluorescence intensity of non U4T anchored control liposome solution. Inset graph is the calibration curve of free CU4T FAM. Black: curve plotted from experimental data; red: fitted curve. (a) Unsaturated liposome (b) Saturated liposome.

2.2.2 Lipid DNA Anchoring to Cell Membrane

Since lipid DNA can be anchored to a variety of liposome membranes, we further challenged the system to tether to a more complicated membrane: cellular membranes. To do this, we incubated HeLa cells with a micellar solution of FAM-modified lipid DNA (U4T23) for 20 min and analyzed cells by flow cytometry after sufficient washing. To rule out nonspecific cellular adsorption and internaliza-

tion of the lipid DNA, a control DNA sequence without lipid tail (CU4T FAM) was measured in addition. Analysis of the FAM emission signal clearly indicated that cells incubated with U4T23 (**Fig. 2.6a, orange**) showed significantly higher fluorescence intensity as compared to CU4T FAM treated control (**Fig. 2.6a, blue**) or untreated cells (**Fig. 2.6a, red**). This significant signal difference highlights the strong and selective interaction of lipid DNA with the cell surface. To evaluate the hybridization feasibility of surface anchored lipid DNA, U4T anchored cells were exposed to CU4T FAM. Flow cytometry data showed that only cells incubated with both U4T and CU4T FAM showed an increased fluorescence signal (**Fig. 2.6b, orange**). In stark contrast, untreated cells (**Fig. 2.6b, red**) and those incubated only with CU4T FAM in the absence of the U4T anchors (**Fig. 2.6b, blue**), revealed considerably lower fluorescence, eliminating nonspecific cellular adsorption or internalization of the CU4T FAM itself as source for the increased signal. Successful anchoring of lipid DNA to another cell line, MDA-MB-468 proved our anchoring method quite universal for cellular membrane modification (**Fig. 2.14**).

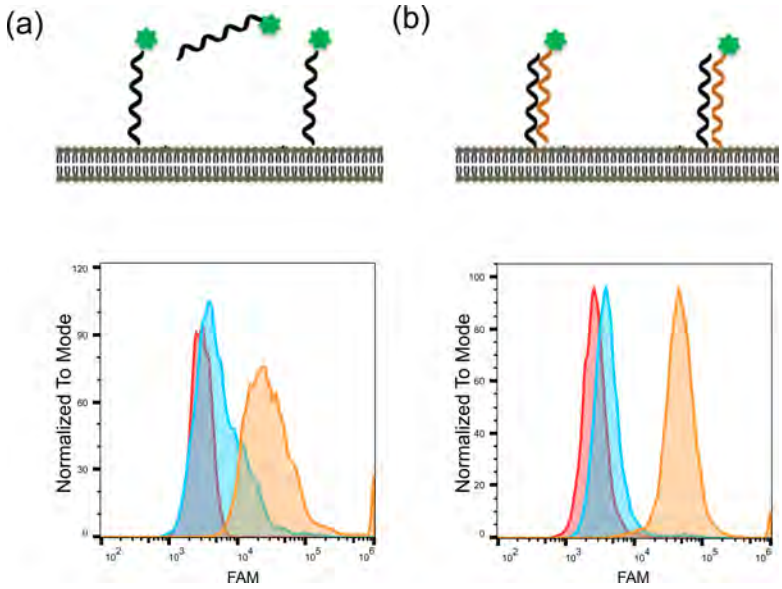

Figure 2.6 | Characterization of lipid DNA anchoring to cell membrane. (a) Top: schematic illustration of anchoring U4T23 on HeLa cells. Bottom: flow cytometry analysis of U4T23 anchoring. HeLa cells were incubated with U4T23 for 20 min before flow cytometry measurement. As a control, cells were also incubated with CU4T FAM for 20 min. Red: untreated control cells; Blue: cells with CU4T FAM; Orange: cells with U4T23. (b) Top: schematic illustration of hybridization of U4T on HeLa cells. Bottom: flow cytometry analysis of U4T hybridization on HeLa cells. HeLa cells were incubated with or without U4T for 20 min, then CU4T FAM was added and after an incubation period of 15 min, flow cytometry measurements were performed. Red: untreated control cells; Blue: cells without U4T; Orange: cells with U4T.

Homogeneous cell membrane distribution of CU4T was unambiguously confirmed by confocal laser scanning microscopy (CLSM), revealing that U4T was uniformly located on the cell membrane and accessible for hybridization (**Fig. 2.7**).

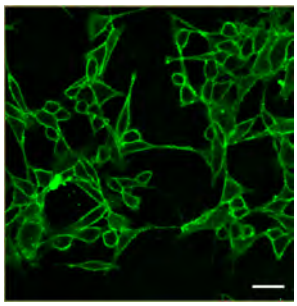

Figure 2.7 | CLSM micrograph of CU4T FAM distribution on U4T anchored HeLa cell membrane. CU4T FAM was incubated with U4T anchored HeLa for 15 min. Scale bar: 40 μm.

Moreover, to demonstrate the hydrophobic interaction strength of the lipophilic tails in lipid DNA and the cellular phospholipid layer, lipid DNA anchoring stability was recorded over time. Therefore, cells were incubated with U4T for different periods of time at 4 °C and hybridized with CU4T FAM afterwards. Subsequent flow cytometry analysis indicated the relative remaining amount of U4T on the cell membrane. Evidently, U4T anchorage was very stable on the cell surface for up to 3 h and there was a minor decrease after 4 h incubation (**Fig. 2.8a**). As low temperature decrease cell viability, thus a longer incubation time period was performed at 37 °C. Surprisingly, even up to 15 h, there was no obvious loss of anchored U4T. The significantly reduced signals for the measurement after 24 h possibly stem from lipid DNA degradation by nucleases in the cell growth medium, cell proliferation, or spontaneous turnover of membrane lipids (**Fig. 2.8b**). To study whether increasing lipid DNA hydrophobicity has an effect on its membrane stability, lipid DNA with six modified deoxyuridine nucleotides (U6T) was synthesized and incubated with cells at 4 °C and 37 °C for the same periods of time as U4T. U6T showed a more stable anchoring than U4T after 4 h incubation at 4 °C (**Fig. 2.8c**). Quite surprisingly, when incubated with cells at 37 °C, a decrease of stability was noticed (**Fig. 2.8d**). This might be an effect of higher cellular toxicity of U6T as compared to U4T (data not shown).

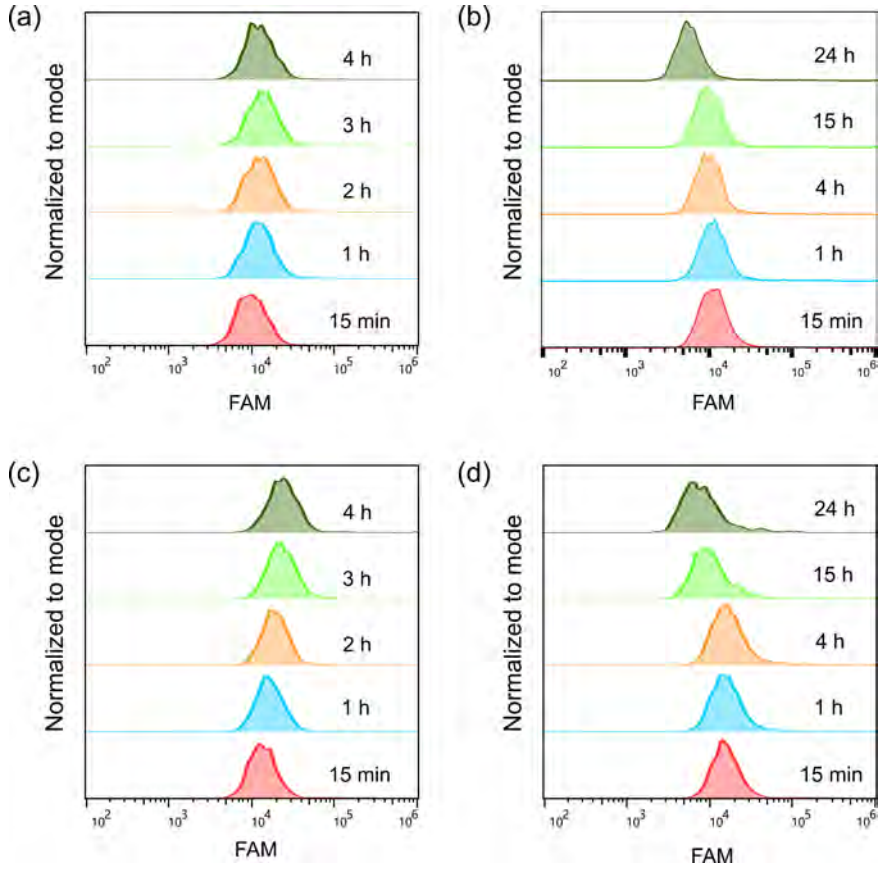

Figure 2.8 | Characterization of lipid DNA membrane anchoring stability. Seeded HeLa cells were incubated with lipid DNA for 15 min, 1 h, 2 h, 3 h or 4 h at 4 °C or incubated for 15 min, 1 h, 4 h, 15 h, or 24 h at 37 °C. Afterwards, each sample was incubated with CU4T FAM for 15 min and subsequently subjected to flow cytometry and CU4T FAM signal was compared. (a) U4T at 4 °C; (b) U4T at 37 °C; (c) U6T at 4 °C; (d) U6T at 37 °C.

Lipid DNA Cellular Toxicity

For any biological application, cellular toxicity is of significant importance and has to be tested before any further steps. Therefore, the effect of the U4T anchor on HeLa cell over 48 h was tested. **Fig. 2.9** indicated that toxicity of U4T is concentration dependent and at up to 10 μM, its effect on cell viability is moderate.

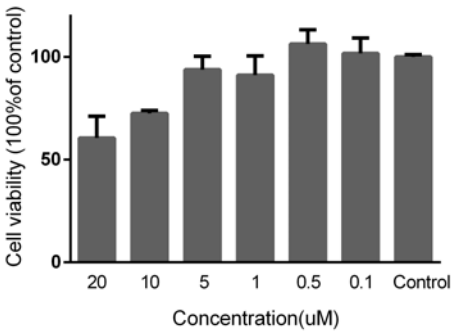

Figure 2.9 | Characterization of toxicity of lipid DNA anchoring to cell membrane. Seeded HeLa cells were incubated with varied concentration of U4T for 48 hours at 37 °C. Afterwards, cell viability was evaluated with XTT assay. Error bars indicate SD of the mean (n = 3).

2.3 Conclusion

Amphiphilic DNA spontaneously inserts into membranes. The driving force is the hydrophobic interactions of the aliphatic chains of nucleobase and the hydrophobic part of the membrane. The nucleic acid moieties of membrane-anchored amphiphilic DNA are free to hybridize with their complementary molecules from the aqueous environment. Hydrophobic moieties of these amphiphilic DNA can be cholesterol molecules[20, 21], single hydrocarbon chains[22, 23] or double hydrocarbon chains[24, 25]. This study here demonstrated that amphiphilic DNA with four hydrocarbon chains can anchor to both saturated (DOPC:DOPE:cholesterol = 2:1:1) and unsaturated liposome membrane (DPPC:cholesterol = 2:1), even to PEGylated formulations. Quantification of these membrane anchored lipid DNA revealed that almost half of input lipid DNA locates in the outer leaflet of liposome and is full accessible to its complementary sequence. It was also observed by confocal microscopy that lipid DNA homogeneously anchors to the cell membrane and this anchoring is applicable to several cell lines. Over time test of cellular membrane lipid DNA reveals a high anchoring stability for several hours. When increasing the hydrophobicity of lipid DNA by adding two more hydrocarbon chains, its membrane anchoring stability is further improved but cellular biocompatibility is compromised.

2.4 Experimental Section

2.4.1 Materials

All chemicals and reagents purchased from commercial suppliers were used without further purification unless noted. 1,2-dioleoyl-sn-glycero-3-phosphocholine (DOPC), 1,2-dioleoyl-sn-glycero-3-phosphoethanolamine (DOPE), 1,2-dipalmitoyl-sn-glycero-3-phosphocholine (DPPC), 1,2-distearoyl-sn-glycero-3-phosphoethanolamine-N-[methoxy(polyethylene glycol)-2000] (ammonium salt) (DSPE-PEG2k), cholesterol (plant derived) and polycarbonate membranes with diameter of 100 nm were acquired from Avanti Polar lipids. Nile red, Triton X-100 was purchased from Sigma Aldrich. Sephadex G-25 column PD-10 was from GE Healthcare. Dulbecco's Modified Eagle Medium (DMEM), fetal bovine serum, and PBS were purchased from Lonza. Lissamine™ Rhodamine B 1,2-Dihexadecanoyl-sn-Glycero-3-Phosphoethanolamine, Triethylammonium salt (rhodamine DHPE), phenol red free DMEM, Penicillin/streptomycin and Trypsin were acquired from Thermo Fisher Scientific. μ-Slide 8 well was obtained from ibidi. HeLa and MDA-MB-468 cell lines and XTT cell proliferation assay kit were purchased from ATCC. All oligonucleotides without lipid modification were purchased from biomers purified by HPLC.

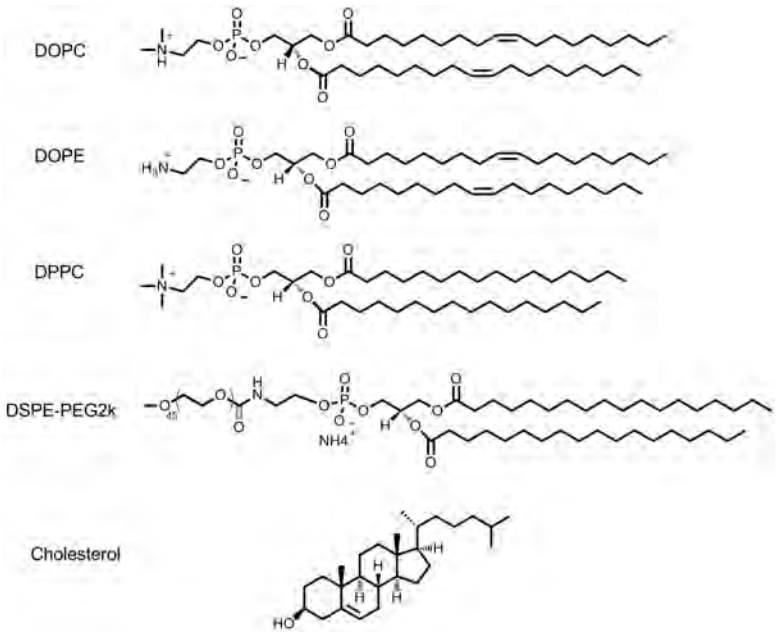

Figure 2.10 | Structures of lipids used in this chapter.

2.4.2 Lipid DNA Synthesis and Characterization

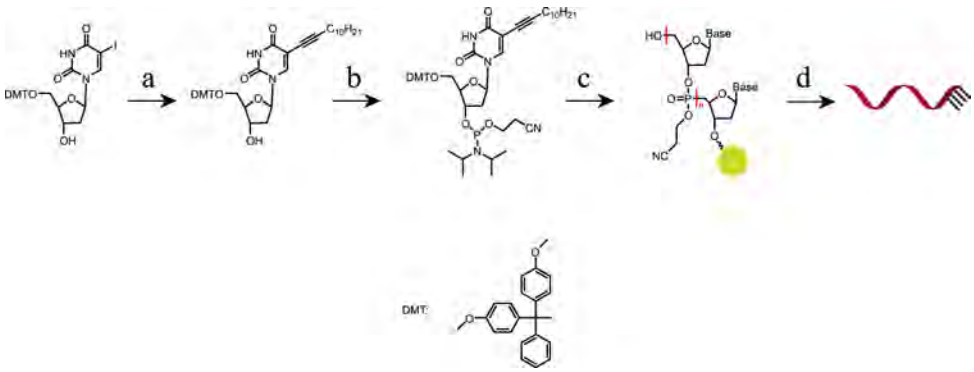

Figure 2.11 | Synthetic steps of lipid-DNA. a: $C_{12}H_{12}$, Palladium-tetrakis(triphenylphosphine), CuI, DIPA, DMF, RT; b: 2-Cyanoethyl N,N-diisopropylchlorophosphoramidite, DIPEA, CH_2Cl_2, RT; c: DNA synthesizer; d: purification.

5-(dodec-1-ynyl) deoxyuracil and 5-(dodec-1-ynyl) deoxyuracil phosphoramidite (**Fig. 2.11**) were synthesized as reported previously.[18] Then the modified uracil

phosphoramidite (0.15 M) was dissolved in acetonitrile, in the presence of 3Å molecular sieves, and the prepared solution was directly connected to a DNA synthesizer (ÄKTA OligoPilot Plus, GE Healthcare (Uppsala, Sweden)). Oligonucleotides were synthesized on a 50 μmol scale using standard β-cyanoethylphosphoramidite coupling chemistry. Deprotection and cleavage from the PS support was carried out by incubation in concentrated aqueous ammonium hydroxide solution overnight at 65 °C. Following deprotection, the oligonucleotides were purified by reverse-phase chromatography, using a C15 RESOURCE RPC 3 mL reverse phase column (GE Healthcare) through a custom gradient elution (A: triethylammonium acetate (TEAAc, 100 mM) and MeCN (5%), B: TEAAc (100 mM) and MeCN (65%)). Fractions were desalted using centrifugal dialysis membranes (MWCO 3000 g·mol^{-1}). For FAM modification, 5'-fluorescein phosphoramidite (Glen Research) was dissolved in MeCN according to manufacturer's recommendation; functionalization was performed using standard β-cyanoethylphosphoramidite coupling chemistry. Oligonucleotide concentrations were determined by UV absorbance using extinction coefficients. Finally, the identity and purity of the oligonucleotides was confirmed by MALDI-TOF mass spectrometry (**Fig. 2.12**).

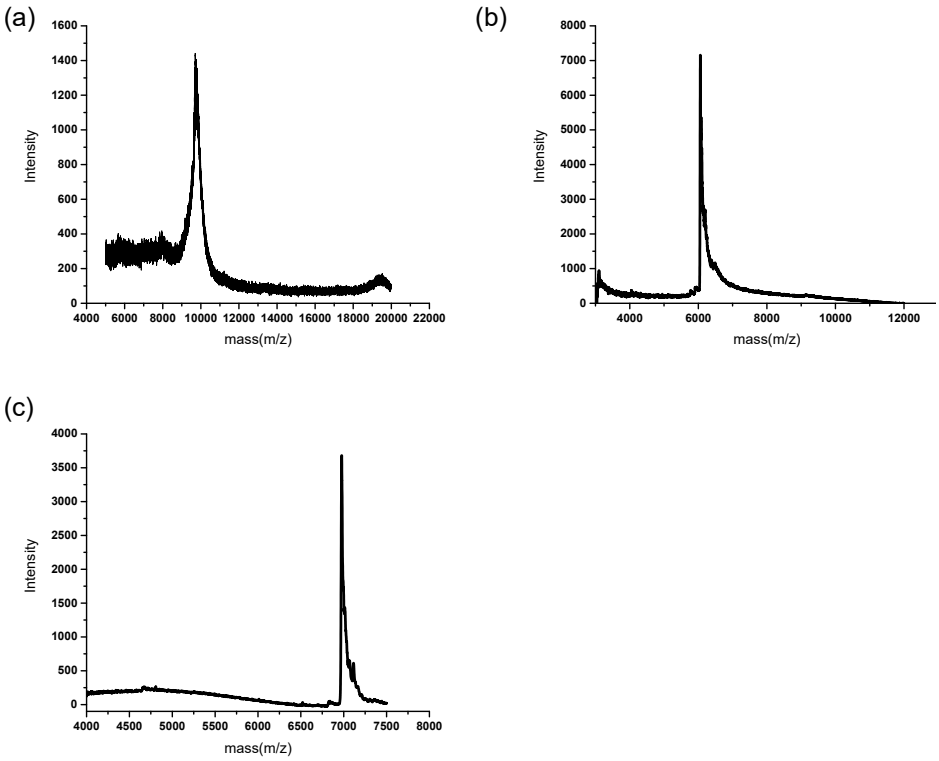

Figure 2.12 | MALDI-TOF mass spectra of lipid-DNA used in the experiments. (a) U4T23 (calcd.: 9314 g·mol^{-1}, found: 9451 g·mol^{-1}), (b) U4T (calcd.: 6033 g·mol^{-1}, found: 6096 g·mol^{-1}), (c) U6T (calcd.: 6915 g·mol^{-1}, found: 6976 g·mol^{-1})

2.4.3 Liposome Preparation

31.23 nmol of U4T in MQ was dried by lyophilisation in a 10 mL glass vial. Then 248 μL mixture of DOPC, DOPE, cholesterol (2:1:1, 10.08 mM) in ethanol or 369 μL mixture of DPPC and cholesterol (2:1, 6.77 mM) in ethanol was added to U4T dry layer. The molar ratio of liposome lipids (cholesterol is not included) with U4T is 80. Ethanol was evaporated by a dry N_2 stream. Dried lipid films were then re-hydrated with PBS buffer. Lipid emulsions were sonicated for 5 min, then subjected to 5 freeze-thaw cycles and 21 times extrusion through a 100 nm polycarbonate membrane by a Mini Extruder (Avanti Polar lipids) at room temperature.

2.4.4 FRET Assay

For FRET analysis of U4T anchoring to DOPC DOPE liposomes, 3% Rhodamine-DHPE was included in the liposome compositions. For FRET analysis of U4T anchoring to DPPC liposome, 3% of Nile red was included in the liposome compositions. Then CU4T ATTO488 was added to the liposome solution at equivalent amount of outside U4T and hybridized using a thermal gradient (40 °C, 15 min; -1 °C per min utill 4 °C). Afterwards, free CU4T ATTO488 was removed by dialysis (Slide-A-Lyzer™ Dialysis Cassettes, 100k) and the emission spectra of CU4T ATTO488 and Rhodamine-DHPE were measured by SpectraMax M3 (Molecular Devices) plate reader. To disassemble the liposomes, 0.3% Triton X-100 was added to the liposome solution and the emission spectra of CU4T ATTO488 and Rhodamine-DHPE was recorded again.

2.4.5 Surface Anchored U4T Quantification

To quantify the amount of lipid DNA on liposome membrane, liposomes with or without U4T anchoring were prepared as described above. CU4T FAM (6.25 nmol) was added to liposome solution (100 μL) to allow overnight hybridization. Unhybridized free CU4T FAM molecules were removed by dialysis. Then purified liposome solution was diluted with PBS and its fluorescence intensity was measured. Fluorescence intensity of a series free CU4T FAM concentrations was also measured resulting in a calibration curve. Then CU4T concentration in the liposome solution was calculated based on this calibration curve.

2.4.6 Calculation of U4T on Liposome

The number of lipids per liposome N_{total} is estimated as outlined below:

$$N_{\text{total}} = 4\pi \frac{\left(\frac{d}{2}\right)^2 + \left(\frac{d}{2} - h\right)^2}{\alpha} \tag{2.1}$$

where d is the diameter of the liposome (outer surface), h is the thickness of the bilayer about 5 nm and α is the lipid head group area. For phosphatidylcholine, α

is about 0.71 nm^2. For unilamellar liposomes, it can be simplified as

$$N_{\text{total}} = 17.69 \times \left[\left(\frac{d}{2} \right)^2 + \left(\frac{d}{2} - h \right)^2 \right] \tag{2.2}$$

For liposomes with a diameter of 100 nm, N_{total} is estimated to be 8×10^4. For lipid DNA and lipid ratio of 80, there are roughly 500 lipid DNA molecules outside per liposome.

2.4.7 Characterization of Lipid DNA Anchored Liposome

To characterize liposomes, DOPC DOPE liposomes were used as a representative liposome composition. Liposomes were prepared as described at a concentration of 5 mM and diluted to 50 μM with PBS and measured with dynamic light scattering and a diameter of 100 nm by intensity was found. As an additional method to show U4T anchoring and membrane hybridization, zeta potential of bare liposomes, U4T anchored liposomes and CU4T ATTO488 hybridized U4T liposomes was measured.

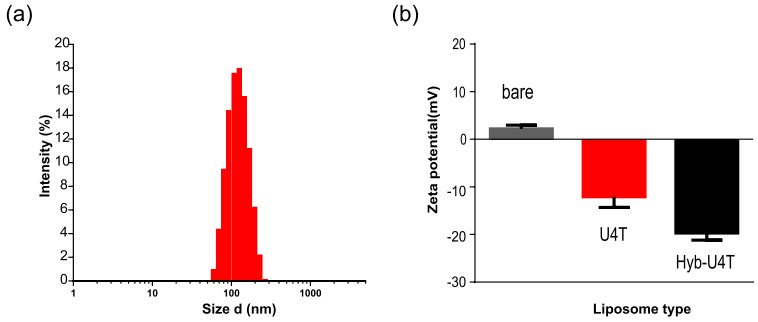

Figure 2.13 | Characterization of liposome. (a) Size distribution of preprared liposome; (b) Zeta potential of different liposome. bare: DOPC DOPE liposome; U4T: DOPC DOPE liposome anchored with U4T; Hyb-U4T: U4T liposome hybridized with CU4T ATTO488.

2.4.8 Cell Culture

HeLa cells were maintained in DMEM supplemented with fetal bovine serum (10%) and penicillin/streptomycin (1%) and cultured at 37 °C with 5% CO_2 and 100% humidity.

2.4.9 Evaluation of Toxicity

All samples were sterilized by 0.22 μm syringe filter before cell experiments. HeLa cells were seeded in a 96 well plate at a density of 1×10^4 per well overnight. Then U4T in PBS solution was added to fresh medium at varied concentrations (in triplicate) then replaced old medium in well plate. After 48 hours, medium was removed and 50 μL of XTT solution pre-mixed with PMS was added to each well. Afterwards, the plate was incubated for 2 hours at 37 °C. Absorbance at 450 nm and 630 nm was recorded.

2.4.10 Anchoring Lipid DNA to Cell Membrane

Confocal Microscopy Sample Preparation: For U4T anchoring, 300 μL HeLa cells were seeded at μ-Slide 8 well overnight and incubated with U4T (4 μM) for 20 min then with CU4T FAM for 15 min. Cells were rinsed with PBS 3 times and replaced with phenol red free DMEM. Imaging was performed on a confocal laser scanning microscope (STP8, Leica) and analyzed by ImageJ.

Flow Cytometry Measurements: For U4T23 anchoring, cells detached to a single cell suspension (10^5 mL^{-1}) were incubated with U4T23 (2 μM) for 20 min. For hybridization experiments on the cell surfaces, after incubation with U4T (4 μM) for 20 min, cells were further incubated with CU4T FAM (4 μM) for 15 min to allow hybridization between U4T on cells and CU4T FAM in solution. After incubation and 3 times rinsing with PBS buffer, cells were measured with the flow cytometer (BD Accuri™ C6, DB Biosciences) with 1×10^4 events collected.

2.4.11 Lipid DNA Stability on Cell Membrane

To test lipid DNA anchoring stability on cell membranes, HeLa cells were seeded at 12 well plate at a density of 1×10^5 overnight. Next day, cells were incubated with U4T or U6T (4 μM) for 15 min, 1 h, 4 h, 15 h, and 24 h at 37 °C. After the desired incubation time, cells were incubated with CU4T FAM (4 μM) for 15 min at 37 °C to allow hybridization. For 4 °C experiments, cells were incubated with U4T or U6T (4 μM) for 15 min, 1 h, 2 h, 3 h, and 4 h at 4 °C then hybridized with CU4T FAM (4 μM) for 15 min at 4 °C. After hybridization, cells were washed 3 times with

PBS and detached before they were subjected to flow cytometry measurements with 10000 events collected.

2.4.12 Hybridization on MDA-MB-468 cell

MDA-MB-468 cells were seeded in 12 well plate and incubated with U4T for 20 mins. After sufficient rinsing with PBS buffer, CU4T FAM was added and hybridization was allowed at 37 °C for 15 min. Cells were then detached, rinsed and subjected to flow cytometry measurement.

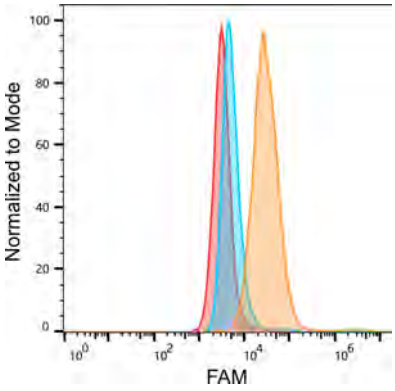

Figure 2.14 | Flow cytometry analysis of DNA hybridization on MDA-MB-468 cells. Red: untreated control cells; Blue: cells without U4T; Orange: cells with U4T.

Bibliography

[1] M. Loew, S. Scolari, A. Herrmann, A. Arbuzova, R. Springer, F. Altenbrunn, O. Seitz, J. Liebscher, D. Huster, J. Am. Chem. Soc. 2010, 132, 16066.

[2] W. Cho, R. V. Stahelin, Annu. Rev. Biophys. Biomol. Struct. 2005, 34, 119.

[3] M. S. Almén, K. J. V. Nordström, R. Fredriksson, H. B. Schiöth, BMC Biol. 2009, 7, 50.

[4] T. Balla, Nature 2016, 529, 292.

[5] M. Hao, F. R. Maxfield, J. Biol. Chem. 2000, 275, 15279.

[6] M. Koval, J. Cell Biol. 2004, 108, 2169.

[7] A. Akbarzadeh, R. Rezaei-sadabady, S. Davaran, S. W. Joo, N. Zarghami, 2013, 1.

[8] L. Sercombe, T. Veerati, F. Moheimani, S. Y. Wu, A. K. Sood, S. Hua, Front. Pharmacol. 2015, 6, 286.

[9] U. Bulbake, S. Doppalapudi, N. Kommineni, W. Khan, Pharmaceutics 2017, 9, 1.

[10] P. Milla, F. Dosio, L. Cattel, Curr. Drug Metab. 2012, 13, 105.

[11] H. Hatakeyama, H. Akita, H. Harashima, Biol. Pharm. Bull. 2013, 36, 892.

[12] M. K. Riaz, M. A. Riaz, X. Zhang, C. Lin, K. H. Wong, X. Chen, G. Zhang, A. Lu, Z. Yang, Int. J. Mol. Sci. 2018, 19.

[13] P. A. Beales, T. Kyle Vanderlick, J. Phys. Chem. B 2009, 113, 13678.

[14] M. Schade, A. Knoll, A. Vogel, O. Seitz, J. Liebscher, D. Huster, A. Herrmann, A. Arbuzova, J. Am. Chem. Soc. 2012, 134, 20490.

[15] I. Pfeiffer, F. Höök, J. Am. Chem. Soc. 2004, 126, 10224.

[16] G. Stengel, L. Simonsson, R. A. Campbell, F. Höök, J. Phys. Chem. B 2008, 112, 8264.

[17] C. Dohno, K. Matsuzaki, H. Yamaguchi, T. Shibata, K. Nakatani, Org. Biomol. Chem. 2015, 13, 10117.

[18] M. Anaya, M. Kwak, A. J. Musser, K. Müllen, A. Herrmann, Chem. - A Eur. J. 2010, 16, 12852.

[19] Z. Meng, J. Yang, Q. Liu, J. W. de Vries, A. Gruszka, A. Rodríguez-Pulido, B. J. Crielaard, A. Kros, A. Herrmann, Chem. - A Eur. J. 2017, 23, 9391.

[20] I. Pfeiffer, F. Höök, J. Am. Chem. Soc. 2004, 126, 10224.

[21] G. Stengel, L. Simonsson, R. A. Campbell, F. Höök, J. Phys. Chem. B 2008, 112, 8264.

[22] A. Rodríguez-Pulido, A. I. Kondrachuk, D. K. Prusty, J. Gao, M. A. Loi, A. Herrmann, Angew. Chemie - Int. Ed. 2013, 52, 1008.

[23] J. J. Benkoski, A. Jesorka, M. Edvardsson, F. Höök, Soft Matter 2006, 2, 710.

[24] N. Dave, J. Liu, Chem. Commun. 2012, 48, 3718.

[25] M. Loew, R. Springer, S. Scolari, F. Altenbrunn, O. Seitz, J. Liebscher, D. Huster, A. Herrmann, A. Arbuzova, J. Am. Chem. Soc. 2010, 132, 16066.